



An experimental and theoretical investigation of the formation of C₇H₇ isomers in the bimolecular reaction of dicarbon molecules with 1,3-pentadiene



Beni B. Dangi^a, Dorian S.N. Parker^a, Ralf I. Kaiser^{a,*}, Daniel Belisario-Lara^b, Alexander M. Mebel^b

^a Department of Chemistry, University of Hawai'i at Manoa, Honolulu, HI 96822, United States

^b Department of Chemistry and Biochemistry, Florida International University, Miami, FL 33199, United States

ARTICLE INFO

Article history:

Received 5 April 2014

In final form 19 May 2014

Available online 26 May 2014

ABSTRACT

We report on the crossed molecular beam reaction of dicarbon, C₂ (X¹Σ_g⁺, a³Π_u), with 1,3-pentadiene (C₅H₈; X¹A') conducted at a collision energy of 43 kJ mol⁻¹ under single collision conditions and studied by *ab initio* and statistical calculations. The reactions involve indirect scattering dynamics initiated by the barrierless addition of dicarbon to the carbon–carbon double bond of 1,3-pentadiene followed by successive rearrangements leading eventually through hydrogen atom elimination to distinct C₇H₇ radical species. The experimental reaction exoergicity of 412 ± 52 kJ mol⁻¹ is consistent with the formation of cycloheptatrienyl, m-tolyl, and/or benzyl radicals predicted as the major products by theory.

© 2014 Elsevier B.V. All rights reserved.

1. Introduction

Resonantly stabilized free radicals (RSFRs) and aromatic radicals (ARs) are considered key reaction intermediates in hydrocarbon flames and in extraterrestrial environments classifying them as important reaction intermediates involved in the mass growth processes and in the formations of polycyclic aromatic hydrocarbons (PAHs) [1–4]. Due to this importance, the role of various C₇H₇ radicals – benzyl (C₆H₅CH₂), o-, m-, p-tolyl (or 2-, 3-, and 4-tolyl) (C₆H₄CH₃), and cycloheptatrienyl (C₇H₇) – have been explored computationally and experimentally [5–7]. Due to the potential key role of the benzyl radical, which is both aromatic and resonance-stabilized, reaction pathways to distinct C₇H₇ isomers have been explored theoretically [6,8,9]. The reaction of methylene (CH₂) with the phenyl radical (C₆H₅), of acetylene (C₂H₂) with the cyclopentadienyl radical (c-C₅H₅) [10], of atomic hydrogen with fulvenallene (C₇H₆) and/or 1-ethynyl-cyclopentadiene (C₇H₆) [5], and of the propargyl radical (C₃H₃) with vinylacetylene (C₄H₄) have been proposed to access various points of the C₇H₇ potential energy surfaces (PESs). Alternatively, bimolecular reactions via C₇H₈ complex formation followed by hydrogen atom elimination might involve reactions of methyl (CH₃) with the phenyl radical (C₆H₅) [8] and of methylene (CH₂) with benzene (C₆H₆) [8]. Similarly, acetylene (C₂H₂) was predicted to react with cyclopentadiene (C₅H₆) via photochemically [2+2] or thermally

induced [4+2] cycloaddition [11]. However, the formation of C₇H₇ isomers – among them the thermodynamically most stable benzyl (C₆H₅CH₂) radical – via the bimolecular reaction of ubiquitous dicarbon molecules (C₂) in their electronic ground (X¹Σ_g⁺) and/or first excited (a³Π_u) states with C₅H₈ isomers such as 1-methyl-1,3-butadiene (1,3-pentadiene, C₅H₈; X¹A') has never been explored. The dicarbon molecule is abundant in hydrocarbon flames and in the interstellar medium [12,13] while the 1-methyl-1,3-butadiene can be formally derived from 1,3-butadiene (C₄H₆) by replacing the hydrogen atom at the C1 carbon atom by a methyl group. 1,3-Butadiene together with its C₄H₆ isomers 1,2-butadiene, 1-butyne, and 2-butyne is omnipresent in combustion flames such as of ethylene [14] and cyclohexane [15]. Distinct C₅H₈ isomers, including 1,3-pentadiene, have been probed in hydrocarbon flames such as of premixed methane/oxygen/cyclopentene [16] and ethylene/oxygen/argon systems [17]. The C₇H₇ species have been identified explicitly via mass spectrometric detection coupled with photoionization in premixed combustion flames of hydrogen/argon/benzene [18], hydrogen/argon/toluene [18], hydrogen/argon/cyclohexane [18], benzene/oxygen/argon [19] and toluene/oxygen/argon [20]. Photoionization efficiency curves suggest the benzyl radical to be the major C₇H₇ species. The benzyl radical is also suggested to be the major intermediate detected in the decomposition of benzylallene [21] and phenylacetic acid [22]. In combustion processes, the benzyl radicals may also form in the high temperature thermal decomposition of mono-substituted aromatics such as toluene, ethylbenzene, propylbenzene, and butylbenzene, which represent primary aromatic surrogates for gasoline, diesel, and jet fuel [23].

* Corresponding author.

E-mail addresses: ralfk@hawaii.edu (R.I. Kaiser), mebela@fiu.edu (A.M. Mebel).

Since the C_7H_7 radicals can reach significant concentrations in combustion flames due to their inherent thermodynamical stability, understanding of their chemistry, in particular their formation and decomposition processes as well as bimolecular reactions, is essential for the development of accurate and predictive combustion engine models. Note that the dicarbon reactions are also relevant for carbon-rich circumstellar environments. For example, Dhanoa and Rawlings implicated dicarbon as a crucial building block in the synthesis of AR and RSFR; therefore, the reaction of dicarbon with 1-methyl-1,3-butadiene may provide a convenient pathway to synthesize C_7H_7 radicals in those environments [24]. However, the formation of these C_7H_7 radicals including the benzyl radical ($C_6H_5CH_2$) via the bimolecular reaction of dicarbon with 1-methyl-1,3-butadiene has to be verified experimentally and computationally. The chemical evolution of macroscopic environments such as combustion flames and the interstellar medium can be best understood in terms of successive bimolecular reactions [10,25–27]. This understanding must be achieved on the molecular level exploiting experiments conducted under single collision conditions, in which the nascent reaction products fly undisturbed toward the detector [28,29]. Very recently, we have shown that the benzyl radical can be synthesized via reaction of dicarbon with 2-methyl-1,3-butadiene (isoprene) [30]. Herein, we report on the results of the crossed molecular beams reaction of dicarbon molecules with the 1-methyl-1,3-butadiene isomer accessing various collision complexes and chemically activated reactive intermediates on the singlet and triplet C_7H_8 surfaces, which then decompose to products including distinct C_7H_7 isomers.

2. Experimental methods

The experiments were conducted under single collision conditions utilizing a universal crossed molecular beam machine [28,31]. Briefly, a pulsed supersonic dicarbon beam, $C_2(X^1\Sigma_g^+, a^3\Pi_u)$, was generated via laser ablation of graphite. A graphite rod was ablated by focusing about 10 mJ per pulse of the output of a Spectra-Physics Quanta-Ray Pro 270 Nd:YAG laser operating at 30 Hz and 266 nm. The ablated species were then seeded in helium carrier gas (99.9999%, Airgas) introduced via a Proch-Trickl pulsed valve operating at repetition rates of 60 Hz. The molecular beam passed a skimmer and a four-slot chopper wheel, which selected a segment of the pulsed dicarbon beam with a well-defined peak velocity of $2087 \pm 55 \text{ ms}^{-1}$ and speed ratio 2.3 ± 0.4 . The segment of the pulsed dicarbon beam then crossed a pulsed 1-methyl-1,3-butadiene (97+%, TCI America) beam perpendicularly in the interaction region. The 1-methyl-1,3-butadiene peak velocity of $721 \pm 15 \text{ ms}^{-1}$ and speed ratio 8.6 ± 0.2 results in a collision energy of $43.2 \pm 1.6 \text{ kJ mol}^{-1}$ and center-of-mass angle $44.4 \pm 1.4^\circ$. The pulsed beam of 1-methyl-1,3-butadiene was prepared by expanding 370 Torr backing pressure via a pulsed valve operating at 60 Hz producing a pressure of about 8×10^{-5} Torr in the secondary source chamber.

The neutral reaction products were analyzed by a triply differentially pumped rotatable mass spectrometer operated in time-of-flight (TOF) mode. Here, the neutral products were ionized by electron impact (80 eV, 2.0 mA), which then passed through a quadrupole mass spectrometer (QMS), and reached a Daly type ion detector [32]. The quadrupole mass spectrometer (Extrel QC 150) passed ions with the desired mass-to-charge (m/z) value. The signal from the photomultiplier tube passed a discriminator and is then fed into a multichannel scaler to record the TOF spectrum [31]. These TOF spectra were recorded at multiple angles and then integrated to obtain the angular distribution of the product(s). A forward-convolution routine was used to fit the experimental

data [33]. This iterative method initially assumes an angular flux distribution, $T(\theta)$, and the translational energy flux distribution, $P(E_T)$ in the center-of-mass frame. Laboratory TOF spectra and the laboratory angular distributions (LAB) were then calculated from the $T(\theta)$ and $P(E_T)$ functions accounting for the velocity and angular spread of each beam. Best fits were obtained by iteratively refining the adjustable parameters in the center-of-mass system within the experimental error limits such as peak velocity, speed ratio, and intensity in the LAB distribution. The ro-vibrational distributions of the singlet ($X^1\Sigma_g^+$) and triplet ($a^3\Pi_u$) electronic states of the dicarbon beam were characterized spectroscopically *in situ* via laser induced fluorescence (LIF), showing the existence of singlet as well as triplet electronic states in our dicarbon beam [28]. Briefly, rotational temperatures (T_{rot}) were measured for the first and second vibrational levels of the first excited electronic state, $a^3\Pi_u$, via the Swan band transition ($d^3\Pi_g - a^3\Pi_u$). The values for $v=0$ and $v=1$ were determined as $T_{\text{rot}} = 240 \pm 30 \text{ K}$ and $190 \pm 30 \text{ K}$ with fractions of 0.67 ± 0.05 in $v=0$ and 0.33 ± 0.05 in $v=1$. The singlet state was probed via the Mulliken excitation ($D^1\Sigma_u^+ - X^1\Sigma_g^+$). At $v=0$ at fractions of 0.83 ± 0.1 , the rotational distribution was bimodal; rotational temperatures were derived to be $T_{\text{rot}} = 200 \text{ K}$ (population fraction 0.44 ± 0.05) and $T_{\text{rot}} = 1000 \text{ K}$ (population fraction 0.39 ± 0.05). At $v=1$ at fractions of 0.17 ± 0.04 , a bimodal rotational distribution was also observed with $T_{\text{rot}} = 200 \text{ K}$ (0.06 ± 0.02) and $T_{\text{rot}} = 1,000 \text{ K}$ (0.11 ± 0.02).

3. Theoretical methods

Stationary points on the singlet and triplet C_7H_8 PES accessed by the reaction of dicarbon, $C_2(X^1\Sigma_g^+/a^3\Pi_u)$, with 1-methyl-1,3-butadiene, including intermediates, transition states, and possible products, were optimized at the hybrid density functional B3LYP level of theory [34] with the 6-311G** basis set. Vibrational frequencies were computed using the same B3LYP/6-311G** method and were used to obtain zero-point vibrational energy (ZPE) corrections. Relative energies of various species were refined employing the coupled cluster CCSD(T) method [35] with Dunning's correlation-consistent cc-pVDZ and cc-pVTZ basis sets [36]. Then the total energies were extrapolated to the complete basis set (CBS) limit using the equation $E_{\text{total}}(\text{CBS}) = (E_{\text{total}}(\text{VTZ}) - E_{\text{total}}(\text{VDZ}) \times 2.5^3/3.5^3)/(1 - 2.5^3/3.5^3)$ [37]. For selected reaction products, we additionally carried out CCSD(T) calculations with the larger cc-pVQZ basis set and extrapolated CCSD(T)/CBS total energies from the CCSD(T)/cc-pVDZ, CCSD(T)/cc-pVTZ, and CCSD(T)/cc-pVQZ values using the following formula, $E_{\text{tot}}(x) = E_{\text{tot}}(\infty) + Be^{-Cx}$, where x is the cardinal number of the basis set (2, 3, and 4) and $E_{\text{tot}}(\infty)$ is the CCSD(T)/CBS total energy [38]. Relative energies discussed in the paper are thus computed at the CCSD(T)/CBS//B3LYP/6-311G** + ZPE(B3LYP/6-311G**) level of theory with two-point (dt) and three-point (dtq) CBS extrapolations and are expected to be accurate within ± 15 and $\pm 10 \text{ kJ mol}^{-1}$, respectively. The B3LYP and CCSD(T) quantum chemical calculations were performed using the GAUSSIAN 09 [39] and MOLPRO 2010 [40] program packages.

Unimolecular rate constants of reaction steps following initial addition of dicarbon to 1-methyl-1,3-butadiene were computed using Rice–Ramsperger–Kassel–Marcus (RRKM) theory [41], as functions of available internal energy of each intermediate or transition state. The internal energy was taken as a sum of the negative of relative energy of a species (the chemical activation energy) and collision energy and one energy level was considered throughout as for a zero pressure limit. For the reaction channels which do not exhibit exit barriers, such as hydrogen atom and methyl eliminations from various C_7H_8 intermediates, we applied the microcanonical variational transition state theory [42] (VTST) and computed variational transition states, so that the individual

microcanonical rate constants were minimized along the reaction paths of the barrierless single-bond cleavage processes. Sums and densities of states required to compute the rate constants were obtained within the harmonic approximation using B3LYP/6-311G** computed frequencies. The rate constants were then utilized to calculate product branching ratios by solving first-order kinetic equations within steady-state approximation.

4. Results

4.1. Laboratory data

Reactive scattering signal from the reactions of dicarbon (C_2 ; 24 amu) with 1-methyl-1,3-butadiene (C_5H_8 ; 68 amu) was observed at $m/z = 91$ ($C_7H_7^+$), $m/z = 90$ ($C_7H_6^+$), and $m/z = 89$ ($C_7H_5^+$) with data at $m/z = 89$ depicting the best signal-to-noise. The TOF spectra at these mass-to-charge ratios were – after scaling – superimposable suggesting that signal at $m/z = 90$ and 89 originated from dissociative ionization of the C_7H_7 product in the electron impact ionizer of the detector. Therefore, our data suggest that only the dicarbon versus atomic hydrogen exchange channel is open, and that the molecular hydrogen loss pathways are closed. We would like to emphasize that in addition to dicarbon, the primary beam also contains atomic carbon and tricarbon molecules; however, tricarbon is unreactive at least at the collision energies of our experiment and hence does not interfere with the scattering signal obtained at lower mass-to-charge ratios. This is evident from the lack of any reactive scattering signal at $m/z = 103$ ($C_8H_7^+$), 102 ($C_8H_6^+$), and 101 ($C_8H_5^+$). Therefore, signal at $m/z = 91$, 90, and 89 cannot originate from dissociative ionization of any reactively scattered products in the tricarbon – C_5H_8 system. Note that the lack of reactivity of tricarbon with unsaturated hydrocarbons has been demonstrated earlier [43] and is associated with substantial threshold energy to reaction based on an entrance barrier and/or the endoergic nature of the reactions. Likewise, ground state carbon atoms would react with the C_5H_8 isomer to products with molecular masses of 79 amu and less; therefore, reactions of carbon do not contribute to scattering signal at $m/z = 91$ to 89. Figure 1a presents selected TOF spectra recorded at various angles in the laboratory frame for the most intense fragment ion $m/z = 89$ ($C_7H_5^+$). These TOF spectra were integrated to derive the laboratory angular distribution (Figure 1b) of the C_7H_7 product(s); this distribution peaks close to the center-of-mass angle of $44.4 \pm 1.4^\circ$. The overall shape depicts a nearly forward–backward symmetric distribution extending at least 40° with the scattering plane defined by both beams. These patterns likely indicate indirect scattering dynamics through the formation of C_7H_8 reaction intermediates on the singlet and triplet surfaces [44]. Finally, we also attempted to record signal for the methyl loss channel at $m/z = 77$ ($C_6H_5^+$), but no reactive scattering signal for the dicarbon– C_5H_8 system was detected; however, as stated above, signal can arise from the reactions of atomic carbon with C_5H_8 forming C_6H_7 ($m/z = 79$), which can then fragment to $m/z = 77$ ($C_6H_5^+$). In summary, the interpretation of the TOF data alone suggests the existence of dicarbon versus hydrogen atom exchange channel(s) and the formation of C_7H_7 isomer(s).

4.2. Center-of-mass functions

We now convert the laboratory data into the center-of-mass (CM) reference frame to obtain the translational energy ($P(E_T)$) and angular ($T(\theta)$) distributions. Laboratory data for the dicarbon plus 1-methyl-1,3-butadiene can be fitted with a single channel (Figure 1) verifying the formation of C_7H_7 isomer(s) (91 amu) plus a hydrogen atom (1 amu). Figure 2a shows that the $P(E_T)$ peaks

slightly away from zero translational energy at around 20 – 30 kJ mol^{-1} suggesting that at least one channel holds a tight exit transition state upon decomposition of the C_7H_8 intermediate(s). Further, the maximum of the translational energy of the $P(E_T)$ resembles the sum of the collision energy plus the reaction energy for those product molecules formed without internal excitation. Therefore, the maximum translational energy release can be utilized to extract the reaction energy. Considering the maximum translational energy of 455 ± 50 kJ mol^{-1} , the reaction is determined to be exoergic by 412 ± 52 kJ mol^{-1} after subtracting the nominal collision energies. Finally, the translational energy distribution helps to calculate the averaged fraction of available energy released into the translational degrees of freedom to be $27 \pm 5\%$; this order of magnitude indicates indirect reaction dynamics [45].

The associated center-of-mass angular distribution, as shown in Figure 2b, is forward–backward symmetric with respect to 90° and is distributed over the complete angular range of 0° to 180° . This finding suggests that this system follows indirect scattering dynamics via the formation of C_7H_8 reaction intermediate(s) holding life times longer than the(ir) rotation period(s) [45,46]. Also, the distribution maximum of the center-of-mass angular distribution at 90° indicates ‘sideways scattering’ and geometrical constraints. In other words, in at least one of the exit channels, the departing atomic hydrogen atom is emitted preferentially perpendicularly with respect to the rotational plane of the decomposing complex, almost parallel to the total angular momentum vector [45].

5. Discussion

In case of complex, polyatomic reactants it is often beneficial to combine the crossed molecular beams data with results from electronic structure calculations (Figures 3 and 4). Let us attempt to identify the reaction product(s) first. Recall that based on the center-of-mass translational energy distribution, the reaction to form C_7H_7 isomers plus atomic hydrogen was found to be exoergic by 412 ± 52 kJ mol^{-1} . A comparison of this data with the results from the electronic structure calculations propose that one or more of the cyclic (aromatic) C_7H_7 isomers are formed: benzyl, o-, m-, p-tolyl, and/or cycloheptatrienyl. The formation of solely non-cyclic C_7H_7 isomers, which are energetically less stable by at least 120 kJ mol^{-1} , can be ruled out. However, we have to concede that based on the experimental data alone, we cannot discriminate which of these isomers – benzyl, o-, m-, p-tolyl, and/or cycloheptatrienyl – is formed. Therefore, we have a closer look at the electronic structure calculations for guidance.

On the triplet PES (Figure 3), dicarbon adds to either C1 or C4 atoms of 1-methyl-1,3-butadiene forming initial complexes **ti1** and **ti2** without barriers. Intermediate **ti1** can decompose to products **tp1** and **tp2**, which are 104 (**99**) and 63 kJ mol^{-1} exoergic relative to the initial reactants as computed at the CCSD(T)/CBS(dt) (CCSD(T)/CBS(dtq)) levels of theory. There is no exit barrier for the hydrogen loss (**tp2**) whereas that for the methyl loss (**tp1**) is 22 kJ mol^{-1} . Otherwise, **ti1** can isomerize to **ti3** by rotation around the C2–C3 bond, to **ti5** by a four-member closure, or to **ti15** by 1,3-H migration. According to our earlier calculations for the analogous $C_2(a^3\Pi_u) + 1,3$ -butadiene reaction [47], the further fate of **ti5** involves an opening of the four-member ring leading to a chain C_7H_8 intermediate and effectively resulting in an insertion of the dicarbon into the C1–C2 bond of 1-methyl-1,3-butadiene; the chain intermediate can further decompose to various chain C_7H_7 isomers by hydrogen eliminations from different positions or to C_6H_5 by methyl loss. However, since rate constant calculations show that the reaction flux from **ti1** to **ti5** is insignificant, we do not pursue these reaction channels further. The intermediate **ti2**

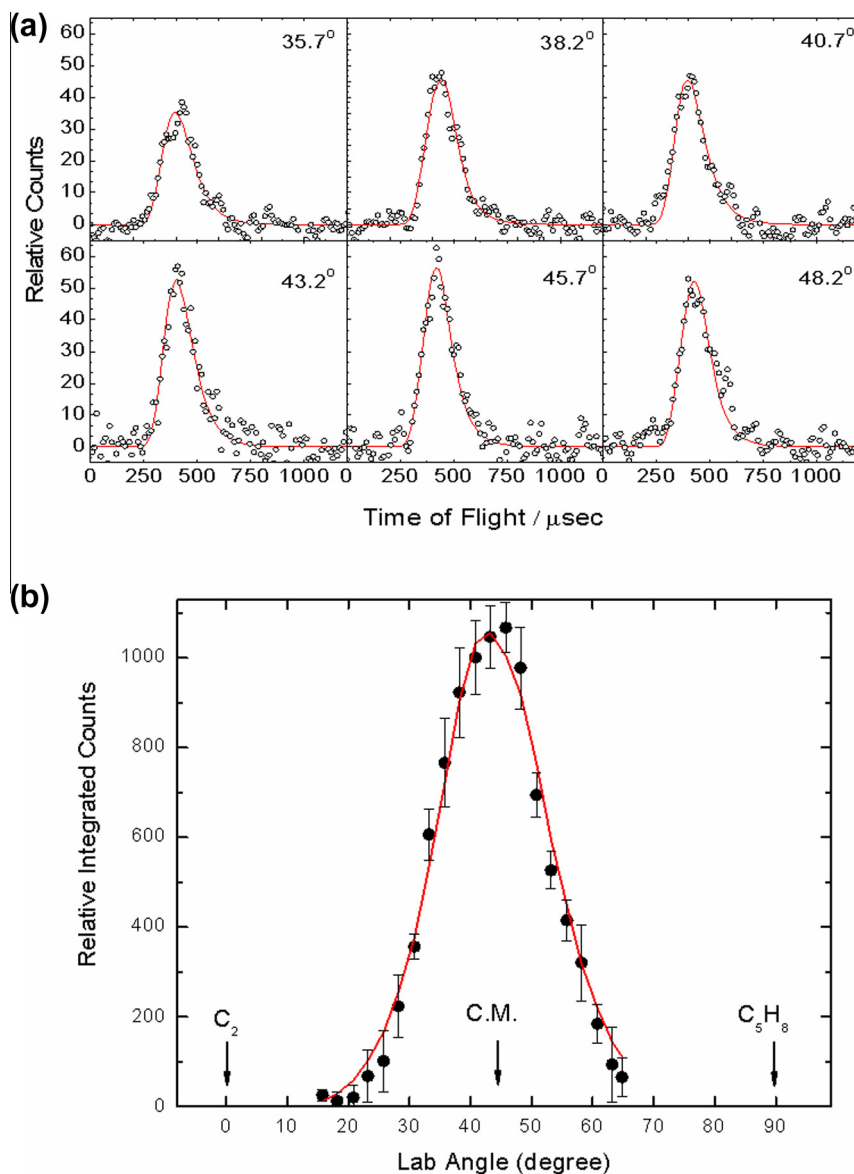


Figure 1. (a) Selected time-of-flight spectra recorded at $m/z = 89$ ($C_7H_7^+$) and (b) corresponding laboratory angular distribution for the reaction of dicarbon (C_2) with 1,3-pentadiene (C_5H_8) forming the C_7H_7 product at a collision energy of 43.2 ± 1.6 kJ mol^{-1} . The circles represent the experimental data, error bars represent the standard deviation and the solid lines represent the fit.

can lose a hydrogen atom from C4 to form **tp3**, undergo a trans-cis conformational change to **ti4** or a four-member ring closure to **ti6**. Similar to **ti5**, **ti6** can further ring-open to a chain C_7H_8 structure and decompose to different acyclic products, but the reaction flux from **ti2** to **ti6** is negligible. According to the computed barrier heights and rate constants **ti1** would mostly dissociate to **tp1** plus methyl or isomerize to **ti3**, whereas **ti2** would nearly exclusively rearrange to **ti4**. The intermediates **ti3** and **ti4** then can easily cyclize to the six-member ring structure **ti7**. The further fate of the **ti7** intermediate is threefold, as it can undergo a 1,2-H shift from the $C(CH_3)H$ group in the ring to the neighboring carbon atom to form **ti9**, a 1,2-H shift from the CH_2 group to **ti8**, or a 1,3-H shift from the methyl group to give **ti17**. The **ti9** structure preferentially loses a hydrogen atom from the CH_2 group producing m-tolyl radical with the overall reaction exoergicity of 383 kJ mol^{-1} , but to a lesser extent may also rearrange to the triplet toluene structure **ti10**. **ti8** may isomerize to **ti10** too, but would preferentially dissociate to phenyl plus methyl (exoergic by 429 (**427**) kJ mol^{-1}) or

o-tolyl plus hydrogen (exoergic by 384 kJ mol^{-1}). A hydrogen shift from the methyl group in **ti8** to the bare ring carbon atom produces **ti18**. The intermediate **ti17**, which can be formed from **ti7** and also from **ti16** via the less kinetically favorable **ti1** \rightarrow **ti15** \rightarrow **ti16** \rightarrow **ti17** and **ti1** \rightarrow **ti3** \rightarrow **ti16** \rightarrow **ti17** routes, can feature 1,2-H migration leading to **ti18** or ring opening to **ti19**. The **ti18** intermediate decomposes to the most thermodynamically favorable product benzyl radical exoergic by 475 (**478**) kJ mol^{-1} by H elimination from the $C(CH_2)H$ group over an exit barrier. A small amount of **ti10**, which can be formed in the reaction, can dissociate to o-, m-, and p-tolyl radicals, to phenyl plus methyl, all via exit barriers, or to the benzyl radical without an exit barrier. There also exists a pathway to the seven-member ring product, cycloheptatrienyl radical. It begins from a conformational change **ti4** \rightarrow **ti11**, then proceeds by 1,7-H migration from the methyl group to the opposite end of the molecule to **ti12**, by seven-member ring closure to **ti13**, by 1,2-H shift to **ti14**, and completes by the H elimination from the remaining CH_2 group to produce

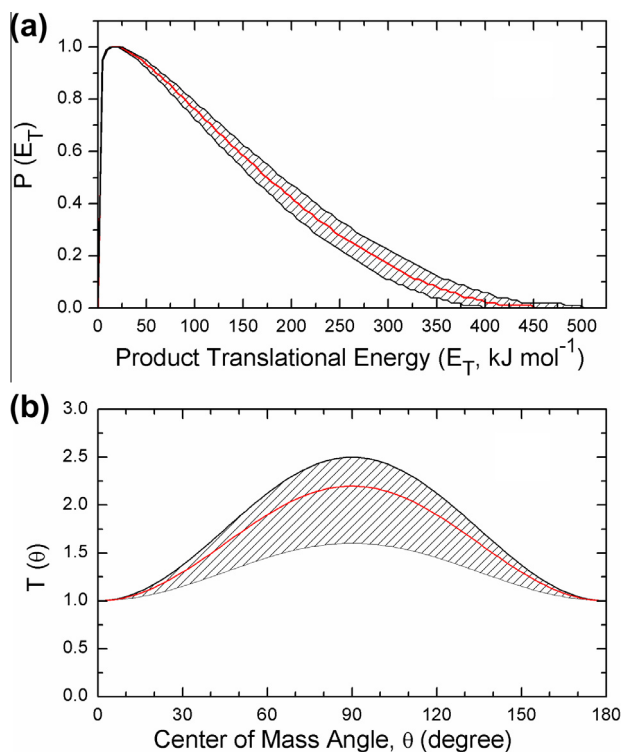


Figure 2. Center-of-mass translational energy flux (a) and angular distribution (b) for the hydrogen atom loss channel leading to C_7H_7 products in the reaction of dicarbon with 1,3-pentadiene. Hatched areas indicate the acceptable upper and lower error limits of the fits and solid red lines define the best-fit functions.

cycloheptatrienyl without an exit barrier and with overall exoergicity of 408 (**411**) kJ mol^{-1} . Here, **ti12** can be also formed from **ti17** via **ti19** by a C–C bond rotation in the latter.

Table 1 presents product branching ratios calculated using RRKM rate constants at collision energies of 0–50 kJ mol^{-1} . Both initial intermediates **ti1** and **ti2** are formed without barriers and the branching of the reaction flux between the two is determined by the dynamics in the entrance channel. Therefore, the branching ratios were computed using either **ti1** or **ti2** as the initial species, or assuming equal probabilities of the dicarbon addition to the C1 and C4 atoms of 1-methyl-1,3-butadiene leading to **ti1** and **ti2**, respectively. If the reaction begins from **ti1**, a large amount of **tp1** is predicted to be produced by a direct CH_3 loss from the initial intermediate. The rest of significant products includes m-tolyl formed via the **ti1** → **ti3** → **ti7** → **ti9** route, cycloheptatrienyl mostly via **ti1** → **ti3** → **ti7** → **ti17** → **ti19** → **ti12** → **ti13** → **ti14**, phenyl plus methyl by the **ti1** → **ti3** → **ti7** → **ti8** mechanism, and benzyl via **ti17** and **ti18**. Alternatively, if the reaction begins with **ti2**, the formation of cycloheptatrienyl is favorable due to the kinetic preference of the **ti2** → **ti4** → **ti11** → **ti12** → **ti13** → **ti14** pathway, followed by benzyl, m-tolyl, and phenyl, with the paths proceeding via the same pivotal **ti7** intermediate. If both **ti1** and **ti2** are formed with equal probabilities in the entrance channel, the reaction products are predicted to include a mixture of cyclic C_7H_7 isomers cycloheptatrienyl, m-tolyl, and benzyl (45:14:9) and the methyl loss products phenyl (8%) and the acyclic C_6H_5 isomer **tp1** (24%). An increase in collision energy should result in a higher yield of **tp1** and a slight growth of the yield of benzyl, whereas the branching ratios of cycloheptatrienyl and m-tolyl decrease by 8–10% in the considered 0–50 kJ mol^{-1} range.

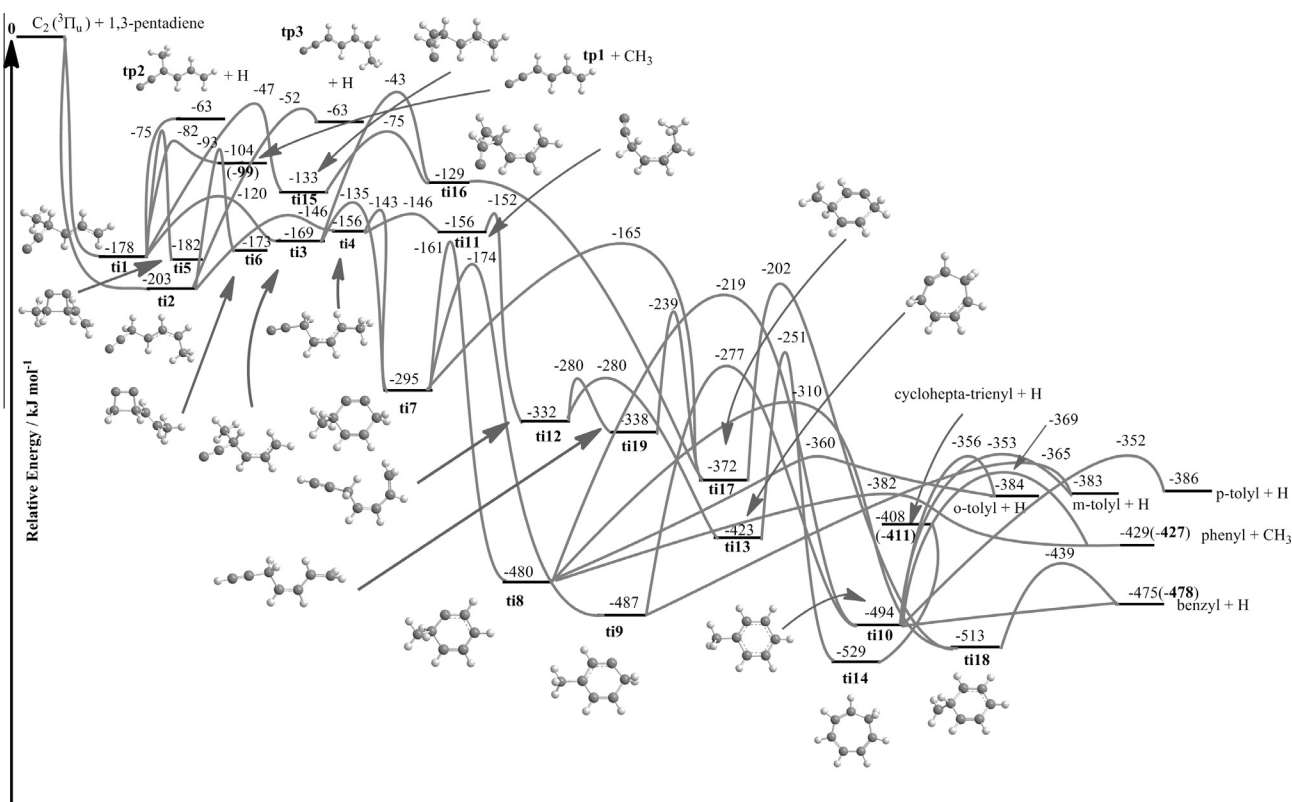


Figure 3. Potential energy surface for the reaction of triplet dicarbon with 1,3-pentadiene calculated at the CCSD(T)/CBS(dt)//B3LYP/6-311G**+ZPE(B3LYP/6-311G**) (plain data) and CCSD(T)/CBS(dtq)//B3LYP/6-311G**+ZPE (B3LYP/6-311G**) (bold data) levels of theory. Intermediates are labeled as **ti** and products as **tp** along with the energies relative to separated reactants in kJ mol^{-1} .

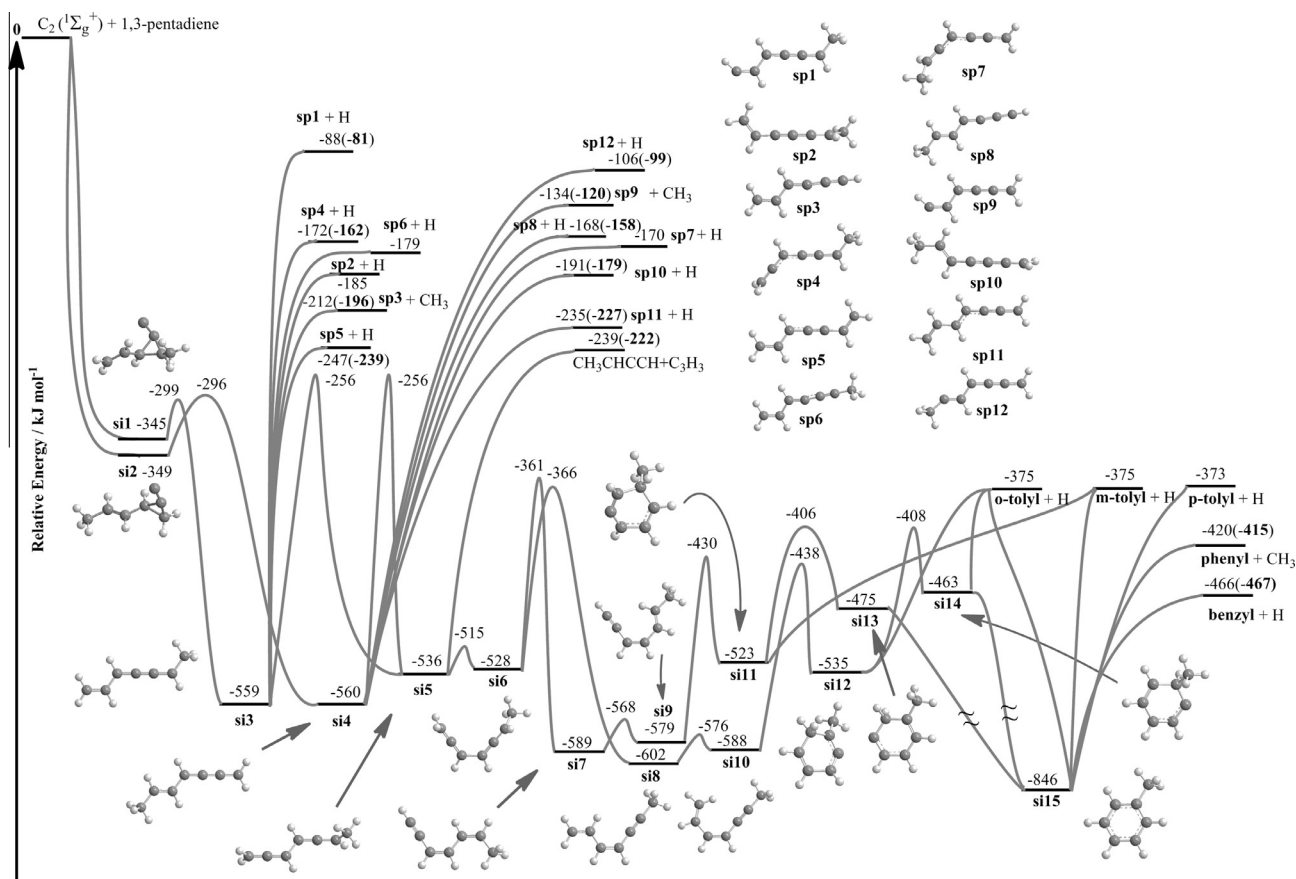


Figure 4. Potential energy surface for the reaction of singlet dicarbon with 1,3-pentadiene calculated at the CCSD(T)/CBS(dt)//B3LYP/6-311G**+ZPE(B3LYP/6-311G**) (plain data) and CCSD(T)/CBS(dtq)//B3LYP/6-311G**+ZPE(B3LYP/6-311G**) (bold data) levels of theory. Intermediates are labeled as **si** and products as **sp** along with the energies relative to separated reactants in kJ mol^{-1} .

Table 1
Branching ratios on the triplet surface (av = averaged).

E_{col} , kJ mol^{-1}	0			10			25			43			50		
	From ti1	From ti2	av												
tp1 + CH_3	16.28	0.07	8.17	22.73	0.11	11.42	33.90	0.19	17.04	47.09	0.31	23.70	51.72	0.37	26.04
ti5	0.10	0.00	0.05	0.13	0.00	0.07	0.18	0.00	0.09	0.24	0.00	0.12	0.26	0.00	0.13
ti6	0.01	0.07	0.04	0.01	0.09	0.05	0.01	0.13	0.07	0.02	0.19	0.10	0.02	0.21	0.11
tp3	0.00	0.00	0.00	0.00	0.01	0.00	0.00	0.02	0.01	0.00	0.04	0.02	0.01	0.06	0.03
o-Tolyl	1.57	0.47	1.02	1.49	0.49	0.99	1.33	0.50	0.92	1.11	0.52	0.81	1.03	0.52	0.77
m-Tolyl	33.08	9.97	21.52	29.67	9.65	19.66	24.32	9.15	16.73	18.48	8.61	13.54	16.51	8.38	12.45
Cyclohepta- trienyl	27.91	74.38	51.14	26.08	73.81	49.94	22.60	72.66	47.63	18.37	71.26	44.82	16.86	70.72	43.79
Benzyl	4.07	9.92	6.99	4.13	10.72	7.42	4.14	12.26	8.20	3.91	14.04	8.97	3.79	14.75	9.27
Phenyl + CH_3	16.99	5.12	11.05	15.76	5.13	10.44	13.52	5.09	9.31	10.78	5.03	7.91	9.80	4.98	7.39

On the singlet surface, dicarbon can barrierlessly add to either C1–C2 or C3–C4 bonds of 1-methyl-1,3-butadiene forming initial complexes **si1** and **si2** (Figure 4). Both **si1** and **si2** subsequently undergo a facile insertion of the C_2 unit into the C1–C2 and C3–C4 bonds leading to the chain C_7H_8 molecules (heptatetraenes) **si3** and **si4**. The intermediate **si3** can decompose by hydrogen and methyl eliminations without exit barriers to six different acyclic products **sp1**–**sp6** with overall exoergicities ranging from 88 (**81**) to 247 (**239**) kJ mol^{-1} as computed at the CCSD(T)/CBS(dt) (CCSD(T)/CBS(dtq)) levels of theory with **sp5** plus atomic hydrogen and **sp3** plus the methyl group being most favorable of them. **si4** can also give rise to six different acyclic products **sp7**–**sp12** exoergic by 106 (**99**)–235 (**227**) kJ mol^{-1} , where **sp11** is

thermodynamically much more favorable than the others. On the other hand, both **si3** and **si4** can undergo a 1,3-H shift to form the same intermediate **si5**. The intermediate **si5** can dissociate by cleaving the central C–C bond to the propargyl + 3-methylpropargyl products exoergic by 239 (**222**) kJ mol^{-1} . Starting from **si5**, the reaction mechanism is very similar to that studied earlier for the $\text{C}_2(\text{X}^1\Sigma_g^+)$ plus 1,3-butadiene reaction [47], with the methyl group playing only a spectator role until the toluene molecule **si15** is formed. The pathways from **si5** to **si15** include the trans-cis conformational change **si5** → **si6**, followed by 1,5-H migrations (**si6** → **si7** or **si6** → **si8**), rotations around single C–C bonds (**si7** → **si9** or **si8** → **si10**), six-member ring closures (**si9** → **si11** or **si10** → **si12**), and two consecutive 1,2-H shifts (**si11** → **si13** → **si15**

Table 2
Branching ratios on the singlet surface (av = averaged).

E_{col} , kJ mol ⁻¹	0			10			25			43			50		
	From si1	From si2	av												
Benzyl	1.91	9.51	5.71	1.85	9.09	5.47	1.75	8.49	5.12	1.64	7.80	4.72	1.60	7.54	4.57
sp5	62.26	0.01	31.13	61.69	0.01	30.85	60.89	0.01	30.45	59.86	0.02	29.94	59.37	0.02	29.69
sp3 + CH ₃	35.49	0.01	17.75	36.09	0.01	18.05	36.92	0.01	18.46	37.98	0.01	18.99	38.48	0.01	19.24
sp11	0.00	88.80	44.40	0.00	89.03	44.52	0.00	89.35	44.68	0.01	89.69	44.85	0.01	89.82	44.91
CH ₃ CHCCH + C ₃ H ₃	0.34	1.67	1.00	0.38	1.86	1.12	0.44	2.14	1.29	0.52	2.48	1.50	0.55	2.61	1.58

or **si12** → **si14** → **si15**). Note that once **si7** or **si8** are produced, the subsequent barriers on the reaction pathways are rather low (and much lower than those in the reverse direction to **si6**) which indicates the reactions forming these intermediates are irreversible and they ultimately lead the reaction flux to **si15**. Also, the **si13** and **si14** intermediates are found to be unstable or metastable; the transition states for their isomerization to **si15** can be found at the B3LYP level but their energies refined at the CCSD(T)/CBS level are either very close or even lower than those of the intermediates indicating that the rearrangement of **si13** or **si14** to **si15** would be nearly spontaneous. Finally, the toluene intermediates can decompose without exit barriers to benzyl exoergic by 466 (467) kJ mol⁻¹, o-, m-, or p-tolyl radicals exoergic by 373–375 kJ mol⁻¹, and phenyl plus methyl exoergic by 420 (415) kJ mol⁻¹.

Table 2 shows product branching ratios on the singlet surface, which were computed with several simplifying assumptions in order to avoid a large number of time-consuming variational RRKM calculations required for single-bond cleavage channels occurring without exit barriers. For **si3** and **si4** we considered only the most favorable channels leading to **sp3**, **sp5**, and **sp11**, while the other hydrogen and methyl loss channels were neglected. This means that the other products among **sp1**–**sp12** can be also formed in principle, but based on the unfavorable energetics and the fact that all reaction steps leading to them exhibit no exit barriers and thus proceed via loose variational transition states, we assume that their relative yields should be insignificant as compared to those of **sp3**, **sp5**, and **sp11**. The second assumption that dissociation of toluene **si15** would predominantly produce the benzyl radical rather than tolyl radicals or phenyl plus methyl is also justified by the much more favorable energy of benzyl and a loose character of all corresponding variational transition states. With these assumptions, we can now analyze the results in Table 2. If the reaction starts from **si1**, the major products are predicted to be **sp5** and **sp3**, which are formed by the H and CH₃ loss from **si3**. However, if the reaction begins from **si2**, the dominant products would be **sp11** and the yield of the benzyl radical would be also significant. If **si1** and **si2** are formed in the entrance channel with equal probabilities, the reaction would produce three major products, **sp11** (45%), **sp5** (30%), and **sp3** (19%), and two minor products, benzyl (5%) and CH₃CHCCH + C₃H₃ (under 2%). The dependence of the calculated branching ration on the collision energy is weak.

Clearly, the singlet reaction alone cannot explain the observations as it mostly produces acyclic C₇H₇ isomers exoergic by 230–240 kJ mol⁻¹ and only ~5% of benzyl exoergic by 467 kJ mol⁻¹, which cannot account for the long tail in the translational energy distribution beyond 283 kJ mol⁻¹. The triplet reaction is computed to form a mixture of cycloheptatrienyl, m-tolyl, and benzyl radicals exoergic by 411 ± 10, 383 ± 15, and 478 ± 10 kJ mol⁻¹, respectively, which is generally consistent with the experimentally determined reaction exoergic of 412 ± 52 kJ mol⁻¹. Moreover, the calculations predict cycloheptatrienyl to be the major C₇H₇ product on the triplet PES and its exoergic shows the best match with the experimental value.

6. Conclusion

We performed the crossed molecular beam reaction of dicarbon, C₂(X¹Σ_g⁺, a³Π_u), with 1,3-pentadiene (C₅H₈; X¹A') at a collision energy of 43 kJ mol⁻¹, which accessed the triplet and singlet C₇H₈ PESs under single collision conditions. The experimental data were combined with *ab initio* and statistical calculations to reveal the underlying reaction mechanism and chemical dynamics. On both the singlet and triplet surfaces, the reactions involve indirect scattering dynamics and are initiated by the barrier-less addition of dicarbon to the carbon–carbon double bond of the 1,3-pentadiene molecule. These initial addition complexes rearrange via multiple isomerization steps leading eventually through atomic hydrogen elimination to the formation of distinct C₇H₇ radical species. The experimentally derived reaction exoergic of 412 ± 52 kJ mol⁻¹ is consistent with the formation of several cyclic C₇H₇ isomers, including o-, m-, and p-tolyl radicals, cycloheptatrienyl, and benzyl, but the calculations predict cycloheptatrienyl, m-tolyl, and benzyl to be the major products on the triplet surface with the branching ratios of 45:14:9. On the singlet surface, mostly acyclic C₇H₇ isomers, such as CH₂CHCHCCHCCH₂ (**sp11**) and CH₂CHCHCCHCCH₂ (**sp5**), are anticipated to be formed with much lower reaction exoergicities of 230–240 kJ mol⁻¹. The calculations predict a significant yield of C₆H₅ products via CH₃ elimination both in the triplet (acyclic CCHCHCCHCCH₂ (**tp1**) and phenyl radicals) and singlet (acyclic CH₂CHCHCCHCCH (**sp3**)) reactions, but these products could not be identified in the experiment due to the interference with the products of the C(³P) + 1,3-pentadiene reaction, as the atomic carbon is also present in the beam.

Acknowledgments

This work was supported by the US Department of Energy, Basic Energy Sciences (Grants no. DE-FG02-03ER15411 to RIK and the University of Hawaii and DE-FG02-04ER15570 to A.M.M. at FIU).

References

- [1] M. Frenklach, *Phys. Chem. Chem. Phys.* 4 (2002) 2028.
- [2] J.A. Miller, S.J. Klippenstein, Y. Georgievskii, L.B. Harding, W.D. Allen, A.C. Simmonett, *J. Phys. Chem. A* 114 (2010) 4881.
- [3] J.A. Miller, M.J. Pilling, E.P. Troe, *Combust. Inst.* 30 (2005) 43.
- [4] J.A. Miller, C.F. Melius, *Combust. Flame* 91 (1992) 21.
- [5] G. da Silva, J.A. Cole, J.W. Bozzelli, *J. Phys. Chem. A* 114 (2010) 2275.
- [6] M. Derudi, D. Polino, C. Cavallotti, *Phys. Chem. Chem. Phys.* 13 (2011) 21308.
- [7] T.C. Zhang et al., *Combust. Flame* 156 (2009) 2071.
- [8] S.J. Klippenstein, L.B. Harding, Y.P. Georgievskii, *Combust. Inst.* 31 (2007) 221.
- [9] V.V. Kislov, A.M. Mebel, *J. Phys. Chem. A* 111 (2007) 3922.
- [10] S. Fascella, C. Cavallotti, R. Rota, S. Carra, *J. Phys. Chem. A* 109 (2005) 7546.
- [11] R.D.J. Froese, J.M. Coxon, S.C. West, K. Morokuma, *J. Org. Chem.* 62 (1997) 6991.
- [12] G.P. Smith, C. Park, J. Schneiderman, J. Luque, *Combust. Flame* 141 (2005) 66.
- [13] H.A. Gueniche, P.A. Glaude, R. Fournet, F. Battin-Leclerc, *Combust. Flame* 151 (2007) 245.
- [14] Q. Zhang, Y.Y. Li, Z.Y. Tian, T.C. Zhang, J. Wang, F. Chinese, Qi, *J. Chem. Phys.* 19 (2006) 379.
- [15] W.J. Li, M.E. Law, P.R. Westmoreland, T. Kasper, N. Hansen, K. Kohse-Hoinghaus, *Combust. Flame* 158 (2011) 2077.
- [16] H.A. Gueniche, P.A. Glaude, R. Fournet, F. Battin-Leclerc, *Combust. Flame* 152 (2008) 245.

- [17] C. Renard, P.J. Van Tiggelen, J.P. Vandooren, *Combust. Inst.* 29 (2002) 1277.
- [18] T. McAllister, J.D. Scott, *Int. J. Mass Spectrom.* 33 (1980) 63.
- [19] B. Yang et al., *P. Combust. Inst.* 31 (2007) 555.
- [20] V. Dettleux, J. Vandooren, *J. Phys. Chem. A* 113 (2009) 10913.
- [21] J.A. Sebree, N.M. Kidwell, T.M. Selby, B.K. Amberger, R.J. McMahon, T.S. Zwier, *J. Am. Chem. Soc.* 134 (2012) 1153.
- [22] F.L. Cozens, W. Ortiz, N.P. Schepp, *J. Am. Chem. Soc.* 120 (1998) 13543.
- [23] R. Sivaramakrishnan, M.C. Su, J.V.P. Michael, *Combust. Inst.* 33 (2011) 243.
- [24] H. Dhanoa, J.M.C. Rawlings, *Mon. Not. R. Astron. Soc.* 440 (2014) 1786.
- [25] J.A. Mulholland, M. Lu, D.H.P. Kim, *Combust. Inst.* 28 (2000) 2593.
- [26] N.W. Moriarty, M.P. Frenklach, *Combust. Inst.* 28 (2000) 2563.
- [27] H. Sabbah, L. Biennier, S.J. Klippenstein, I.R. Sims, B.R. Rowe, *J. Phys. Chem. Lett.* 1 (2010) 2962.
- [28] R.I. Kaiser et al., *Faraday Discuss.* 147 (2010) 429.
- [29] P. Casavecchia, N. Balucani, G.G. Volpi, *Annu. Rev. Phys. Chem.* 50 (1999) 347.
- [30] B.B. Dangi, D.S.N. Parker, T. Yang, R.I. Kaiser, A.M. Mebel, *Angew. Chem., Int. Ed.* 53 (2014) 4608.
- [31] Y. Guo, X. Gu, E. Kawamura, R.I. Kaiser, *Rev. Sci. Instrum.* (2006) 77. 034701/1-034701/9.
- [32] N.R. Daly, *Rev. Sci. Instrum.* 31 (1960) 264.
- [33] Weiss, P. S. University Of California, Berkeley, 1986.
- [34] C.T. Lee, W.T. Yang, R.G. Parr, *Phys. Rev. B* 37 (1988) 785.
- [35] G.D. Purvis III, R.J. Bartlett, *J. Chem. Phys.* 76 (1982) 1910.
- [36] T.H. Dunning Jr., *J. Chem. Phys.* 90 (1989) 1007.
- [37] S.B. Huh, J.S. Lee, *J. Chem. Phys.* 118 (2003) 3035.
- [38] K.A. Peterson, T.H. Dunning, *J. Phys. Chem.* 99 (1995) 3898.
- [39] Frisch, M.J. et al.: GAUSSIAN 09, Revision A.1. Gaussian Inc: Wallingford CT, 2009.
- [40] Werner, H.-J.; Knowles, P. J.; Kinizia, G.; Manby, F. R.; Schutz, M.; Celani, P.; Korona, T.; Lindh, R.: MOLPRO, version 2010.1, a package of *ab initio* programs. 2010.
- [41] P.J. Robinson, K.A. Holbrook, *Unimolecular Reactions* (1972).
- [42] D.G. Truhlar, B.C. Garrett, *Acc. Chem. Res.* 13 (1980) 440.
- [43] X.B. Gu, Y. Guo, A.M. Mebel, R.I. Kaiser, *Chem. Phys. Lett.* 449 (2007) 44.
- [44] Y.T. Lee, *Science* 236 (1987) 793.
- [45] R.D. Levine, *Molecular Reaction Dynamics*, Cambridge University Press, Cambridge, UK, 2005.
- [46] R.I. Kaiser, C. Ochsenfeld, M. HeadGordon, Y.T. Lee, A.G. Suits, *Science* 274 (1996) 1508.
- [47] F.T. Zhang, B. Jones, P. Maksyutenko, R.I. Kaiser, C. Chin, V.V. Kislov, A.M. Mebel, *J. Am. Chem. Soc.* 132 (2010) 2672.